Please cite the attached paper as follows:

Doorly, N., Irving, K., McArthur, G., Combie, K., Engel, V., Sakhtah, H., Stickles, E., Rosenblum, H., Gutierrez, A., Root, R., Liew, C-W. and J.H. Long, Jr. (2009). Biomimetic evolutionary analysis: robotically-simulated vertebrates in a predator-prey ecology. *Proceedings of the 2009 IEEE Symposium on Artificial Life*, 147-154.

Biomimetic Evolutionary Analysis: Robotically-Simulated Vertebrates in a Predator-Prey Ecology

Nicole Doorly, Kira Irving, Gianna McArthur, Keon Combie, Virginia Engel, Hassan Sakhtah, Elise Stickles, Hannah Rosenblum, Andres Gutierrez, Robert Root, Chun Wai Liew, and John H. Long, Jr.

***Abstract*—To test adaptation hypotheses about the evolution of animals, we need information about the behavior of phenotypically-variable individuals in a specific environment. To model behavior of ancient fish-like vertebrates, we previously combined evolutionary robotics and software simulations to create autonomous biomimetic swimmers in a simple aquatic environment competing and foraging for a single source of food. This system allowed us to test the hypothesis that selection for improved forage navigation drove the evolution of stiffer tails. In this paper, we extend our framework to evaluate more complex environments and hypotheses. Specifically, we test the hypothesis that predator-prey dynamics and the need for effective foraging strategies, operating simultaneously, were key selection pressures driving the evolution of morphological and sensory traits in early, fish-like vertebrates. Three evolvable traits were chosen because of their importance in propulsion and predator avoidance: (1) the number of vertebrae in the axial skeleton, (2) the trailing edge span of the caudal fin, and (3) the sensitivity of the sensory lateral line. To produce variable offspring, we used a genetic algorithm that rewarded parents with high fitness, allowing them to mate randomly and combine their mutated gametes. Offspring were then instantiated as autonomous embodied robots, the prey. These prey were chased by a non-evolving autonomous predator. Both kinds of robots were surface swimmers. The prey used a control architecture based on that of living fish: a two-layer subsumption architecture with predator escape over-riding steady swimming during foraging. The performance of six different prey robots in each generation was judged with a relative fitness function that rewarded a combination of high speed, rapid escape acceleration, escape responses, and the ability to stay away from the predator while at the same time staying close to the food source. This approach, which we call biomimetic evolutionary analysis, shows promise for investigators seeking new ways to test evolutionary hypotheses about biological systems.**

This work was funded by the U.S. National Science Foundation (DBI-0442269 and BCS-0230764).

N. Doorly was with the Interdisciplinary Robotics Research Laboratory and the Cognitive Science Program, Vassar College, Poughkeepsie, NY 12604 USA. She is now with the Mechanical and Aerospace Engineering Department, Case Western University, Cleveland OH 44106 USA. (email: ncdoorly@gmail.com).

K. Irving was with the Neuroscience and Behavior Program, Vassar College, Poughkeepsie, NY 12604 USA. She is now with the Neuroscience Institute, Stanford University School of Medicine, Stanford, CA 94305 USA. (email: kirving@stanford.edu).

G. McArthur was with the Department of Biology, Vassar College, Poughkeepsie, NY 12604 USA. She is now with the Memorial Sloan-Kettering Cancer Center, New York, NY 10021 USA. (email: gnm316@aol.com).

K. Combie was with the Biochemistry Program, Vassar College, Poughkeepsie, NY 12604 USA. He is now with the College of Medicine, Howard University, Washington, DC 20059 USA. (email: keoncombie@gmail.com).

V. Engel was with the Department of Biology, Vassar College, Poughkeepsie, NY 12604 USA. She is now with the School of Oceanography, University of Washington, Seattle, WA 98028 USA. (email: virginia.engel@gmail.com).

H. Sakhtah is with the Biochemistry Program, Vassar College, Poughkeepsie, NY 12604 USA. (email: hasakhtah@vassar.edu).

E. Stickles is with the Independent Program, Vassar College, Poughkeepsie, NY 12604 USA. (email: elstickles@vassar.edu).

H. Rosenblum is with the Department of Biology, Vassar College, Poughkeepsie, NY 12604 USA. (email: harosenblum@vassar.edu).

A. Gutierrez is with the Department of Biology, Vassar College, Poughkeepsie, NY 12604 USA. (email: angutierrez@vassar.edu).

R. Root is with the Department of Mathematics, Lafayette College, Easton, PA 18042 USA. (email: robroot@lafayette.edu).

C. W. Liew is with the Computer Science Department, Lafayette College, Easton, PA 18042 USA. (email: liew@cs.lafayette.edu).

J. H. Long, Jr. is a member of IEEE and is with the Interdisciplinary Robotics Research Laboratory, the Department of Biology, and the Cognitive Science Program, Vassar College, Poughkeepsie, NY 12604 USA (corresponding author; phone: 845-437-7305; fax: 845-437-7315; email: jolong@vassar.edu).

I. Introduction

As a modeling approach within the multidisciplinary field of artificial life (AL), evolutionary robotics (ER) uses selection — feedback from the environment to a population of agents through a predetermined fitness function — to adapt physically-embodied or digitally-simulated agents without on-going intervention from an investigator [13]. Targets of selection include control systems and hardware. Using robotic or digital simulations, ER finds novel solutions in high-parameter search space that locally optimize agents' (1) behavior, (2) learning, and/or (3) structure-function relationships [13]. Inspired by the success of ER and the biocentric goals of AL, we combine the two with one purpose — to test adaptation hypotheses about organismal evolution. We call this approach biomimetic evolutionary analysis (BEA).

Using BEA, we previously tested the hypothesis that increased tail stiffness of early fish-like vertebrates, mediated by changes in the axial skeleton, was an adaptation for improved foraging [12]. Selection on foraging in a population of surface-swimming autonomous robots improved navigational prowess, an index of behaviors related to quickly finding and holding station about a food source. Navigational prowess, in turn, was positively correlated with increased spring stiffness of the tails: variation in tail stiffness explained 40% of the variance in navigational prowess. We have also begun to develop

physics-based digital simulations of our robots to test the same hypothesis [11].

While we recognize that it is impossible to know exactly how adaptation occurred in the past, model simulations can falsify an adaptation hypothesis by demonstrating low plausibility of the purported selection pressure. One criticism of our work is that we are likely to find other selection pressures that are equally or more plausible than foraging. A second criticism is that having a single target of selection — tail stiffness — constrains the possible evolutionary outcomes, which are always contingent upon the interactions of correlated traits. A third criticism is that our model of a vertebrate is overly-simplistic.

In response, we created a new robotic simulation that tests a different selection pressure for character evolution in early fish-like vertebrates: a predator pursuing a prey [8, 14]. Also, we present three targets upon which selection can act simultaneously, three traits that evolved in early vertebrates [9]: (1) number of vertebrae (proportional to tail stiffness), (2) span of the caudal fin (proportional to hydrodynamic power output), and (3) the sensitivity of the lateral line to predators (related to local fluid disturbances). We chose these features because they are thought to be critical biomechanical and sensory traits that enhance performance in aquatic foraging and predator avoidance [10, 12]. Finally, we made the new robots more complex, adding additional biomimetic sensory systems and behaviors. We note that predator-prey experiments have proven to be extremely effective in embodied evolutionary robotics [4, 5, 16].

In our evolutionary simulation, we select for individual prey robots who show enhanced performance in both foraging and predator avoidance relative to the performance of other individuals in a given generation. Selection is codified by a compound fitness function that permits multiple successful strategies to evolve (see Methods). The adaptation hypothesis we test is that selection for enhanced foraging and predator avoidance will increase, over generational time, the population's mean number of vertebrae, mean span of the caudal fin, and the mean predator detection sensitivity. This hypothesis is falsified if we find either (1) no change in the population mean of these traits over generational time or (2) a decrease in the population mean of the traits over generational time.

II. Methods

A. Embodied Robots

We built two fully autonomous surface-swimming robots — predator and prey — each with different hardware components and behavior that allowed them to engage in a pursuit-escape interaction. Only traits of the prey robot were evolved; the sole function of the predator robot was to be an agent of selection. The behavior architecture for both prey and predator were implemented as computer programs written in Interactive C and downloaded onto a microcontroller (MIT HandyBoard, Newton Labs, Renton, WA) onboard the robot (code available upon request). All sensors and motors were connected *via* ports on the microcontroller.

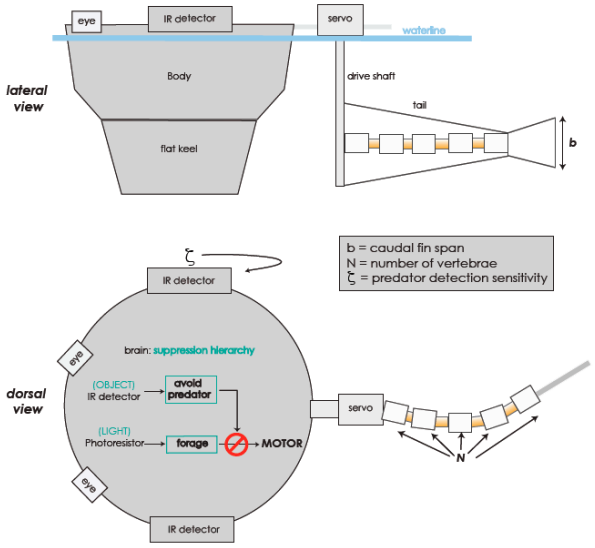

Fig. 1. Design of the surface-swimming prey robot. Lateral and dorsal views, including diagram of suppression hierarchy of software [1]. Note that the prey has two sensory systems: (a) visual, in the form of simple photoresistors acting as eyes for directional navigation up a light gradient, and (a) lateral line, in the form of IR proximity detectors acting to detect nearby predators. As occurs in living fish, the escape response triggered by the IR detectors over-rides the forage navigation mediated by the photoresistors. The skeleton of the tail is a biomimetic vertebral column. The three evolvable traits are shown: *b*, the caudal fin span, *N*, number of vertebrae, and ζ, predatory detection threshold.

Prey (Fig. 1): Sensors on the prey robot were meant to mimic selected functions of eyes and lateral lines in fish: (1) two forward-mounted photoresistors (cadmium sulphide, Radio Shack, USA) and (2) two side-mounted IR proximity detectors (GP2D02, Sharp Electronics, USA). The difference in light intensity at the photoresistors controlled foraging for light, a proxy for food, by calculating a lateral offset angle for the propulsive tail. Either side-mounted IR proximity detector could trigger an escape response that suppressed steady swimming, used the tail to initiate a large-amplitude flick that rotated the robot in the direction opposite to the stimulus, followed by a propulsive flick of the tail before resuming foraging. Motor output was meant to mimic steady oscillator propulsion controlled by central pattern generators and escape responses controlled by reticulospinal neurons in fish [6]. A single servo motor (MPI MX-400, Maxx Products, Lake Zurich, IL, USA) drove propulsion of the attached biomimetic tail. During foraging, the servo generated a steady, 2 Hz, ± 0.44 radian oscillation of the attached tail, with lateral offset for turning determined by the photoresistors. During escape, the servo generated a single maximal rotation of up to 3.14 radians, depending on its starting offset position, followed by a pause of 0.5 seconds to allow rotation, followed by another rotation of the tail, of 1.57 radians, to accelerate the robot forward. To allow detection by the predator, the prey

carried an IR beacon with four cardinal-direction transmitters (Pololu Inc., Las Vegas, NV, USA).

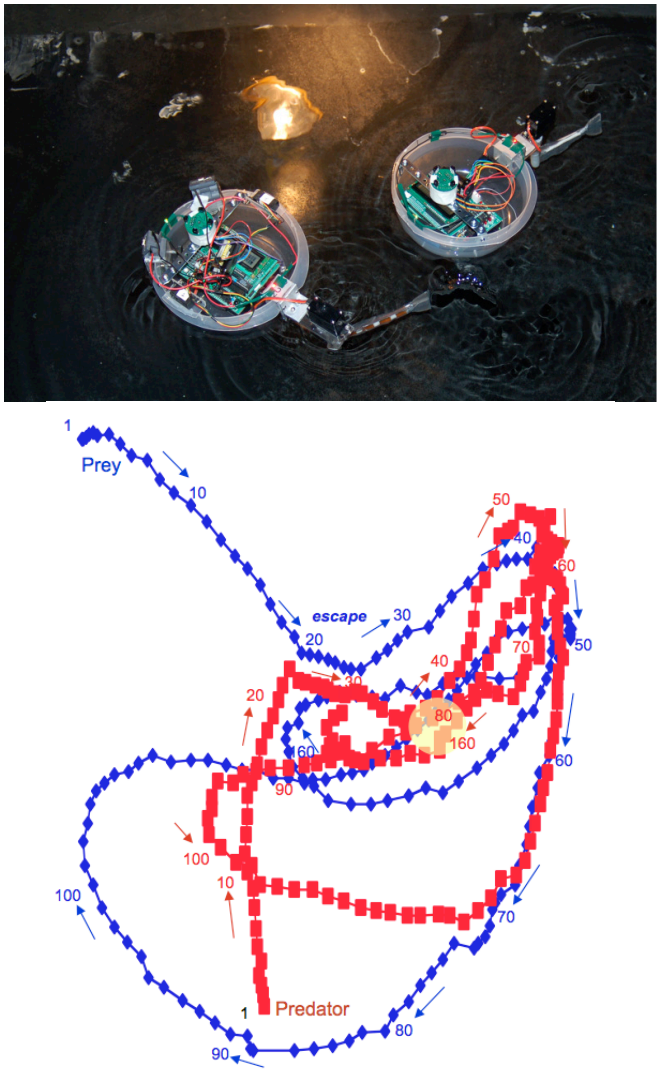

Fig. 2. Selection in action. TOP: The prey robot (left) initiates an escape in response to the presence of the predator (right). The tail of the prey, an biomimetic axial skeleton containing vertebrae (white elements), is one morphological structure whose evolution we seek to understand. BOTTOM: Trajectories of predator and prey robots during a three-minute evolutionary trial (Generation 1, trial 2 of 18). Each point plots positions of the robots at 1 s intervals, indicated by the numbers. Note initially that the prey heads straight for the light source (yellow disk) and that the predator heads straight for prey. The first escape response, at 20 s, is noted.

Predator (Fig. 2): Sensors of the predator robot were meant to mimic the function of a visual predator able to see and track a prey: an array of four directional IR receivers that calculated the bearing of the prey by signal intensity differences from the prey's IR beacon. Heading of the predator was adjusted to null the bearing. The motor output of the predator was identical to that of the prey in terms of steady swimming and offset adjustments for turning. The predator swam with a flexible tail built in an identical manner to the tail for prey (see below), except with a rubber central axis. Neither the predator nor its tail evolved over the course of the experiment.

B. Evolvable Traits

Based on the fossil record of vertebrates [10], three traits were chosen as possible targets of selection: number of vertebrae, N, span of the caudal fin, b, and predator detection threshold, ζ. N and b are important functional elements of the biomimetic, propulsive tail, with N proportional to the spring stiffness of the tail and b proportional to the hydrodynamic power output. Defined ranges of possible values for these traits are shown in Table 1. N and b were morphological traits that required us to build unique tails for each genotype; we built a total of 90 tails (5 generations x 6 individual genotypes x 3 replicates of each genotype). ζ was a trait determined by software that could be reprogrammed for each trial.

TABLE 1
RANGE OF VALUES FOR PHENOTYPIC TRAITS

Symbol	Phenotypic Trait	Range
b	span of caudal fin	0 to 50 mm
N	number of vertebrae	2 to 13
ζ	predatory detection threshold	10 to 60 cm

Each tail was built around a hydrogel that served as a mimic of the vertebrate notochord, matching real material properties [12]. Hydrogels were made of a 0.1 g l^{-1} of gelatin (porcine skin, Type A, Sigma, St. Louis, MO, USA) dissolved in heated, distilled water and poured into custom-built molds in the shape of a right, circular cylinder with a 1.0 cm inner diameter. After cooling at 6° C, the gelatin hydrogels were cross-linked with 2.5% glutaraldehyde (EM grade, Polysciences, Warrington, PA) in a phosphate buffer solution at pH 7.0 for four hours. Finally, the hydrogels were rinsed for 30 minutes in two separate distilled water baths to remove unreacted glutaraldehyde. To minimize any effects of aging, we tested all hydrogels within 24 hours after fixation.

Vertebrae were machined hollow circular cylinders made of Delrin™ (DuPont, Inc., USA). Depending on the number needed for a particular individual, elements were slid onto the hydrogel and affixed in even spacing using cyanoacrylic glue (Fig. 1). Caudal fins were trapezoids cut from 3mm thick Lucite™ (Lucite International, Southhampton, UK) with a variable trailing edge span, b, depending on the size needed for a particular individual. Each caudal fin was attached using hot glue to the terminal vertebra of the vertebral column. To the proximal end of the vertebral column we attached a rectangular piece of Lucite™ that inserted into a Delrin™ driving shaft attached to the servo motor. To finish the tail, the composite structure was placed in a bilayer of Press'n Seal™ (Glad, Inc., USA), cut as a vertical septum to support the tail in the dorsoventral plane without adding to lateral stiffness. The final evolvable trait, ζ, was a property of the IR detectors used as the lateral line (see previous section), with distance to target adjusted as needed for each new individual.

C. Evolutionary Experiments

A population of 18 individual prey robots was tested each

generation. The 18 individuals were of six different phenotypes, each with three clones. Clones were used to provide replication for statistical power, and since each clone was independently fabricated, they represented independent data points. The individuals were tested in random order relative to their phenotypes. We ran six generations of experiments; upon analysis of the video of the sixth generation we noticed mechanical problems with our robots. The experiments were terminated; we discarded selection data from the sixth generation that would have allowed us to determine offspring of the seventh generation.

Each individual was tested against the predator for a three-minute trial in a 3-m diameter tank. The trial was videotaped from a stationary location directly above the tank (JVC digital video camcorder; 30 Hz temporal resolution; 1 cm spatial resolution at 3 m). In the center of the tank hung an incandescent light source (100 W) positioned 1 m above the water's surface to provide a 1-m diameter cone of projection on the surface. This was the only light source in the laboratory, and the walls of the tank and the room had been painted matte black to reduce incidental reflections. In addition to ballast to adjust trim, the prey robot carried a wireless three-axis translational accelerometer (Wireless Dynamics Sensor System, Vernier Software & Technology. Inc., Beaverton, OR, USA). We swam the prey solo to measure peak composite acceleration (vector sum of sway and surge acceleration) during escapes (1000 Hz sample rate). Each individual was tested six times, three times escaping to the left and three times to the right. The mean of the peak values from each trial was used.

For each trial, bow and stern LED markers on the predator and prey were manually digitized at 1 s intervals (LoggerPro v. 3.5; Vernier Software & Technology. Inc., Beaverton, OR, USA). We then calculated a mid-point to use as the position of each robot. From these positional data, we calculated five performance properties for each prey robot: (1) mean swimming speed, u (m s^{-1}), along the trajectory, (2) mean distance from the light source, R (m), (3) mean distance from the predator, D (m), and (4) number of escape responses, θ. From the acceleration trials, we measured the prey's peak acceleration during escapes, a (m s^{-2}).

D. Fitness Function

To compute relative evolutionary fitness, mean values of the six performance variables for the three clones of the six individual phenotypes were compared to the means of the population for that generation. The relative fitness, ω_{ij}, of individual i in generation j was calculated:

$$\omega_{ij} = \frac{u_{ij} - \bar{u}_j}{s_{u_j}} - \frac{R_{ij} - \bar{R}_j}{s_{R_j}} + \frac{D_{ij} - \bar{D}_j}{s_{D_j}} + \frac{a_{ij} - \bar{a}_j}{s_{a_j}} + \frac{\theta_{ij} - \bar{\theta}_j}{s_{\theta_j}}$$

where s is the standard deviation of the population. Thus the deviation of each individual from the mean was normalized by the standard deviation of the population, creating a z-score for each individual's variables, with the sum of the z-scores creating the individual's relative fitness. The individuals with the top three relative fitness scores were awarded six, four, and two gametes, respectively, for the gene pool.

Individuals in the population were selected based on their ability to avoid predators and forage successfully. Selecting for these behaviors imposes different, and perhaps conflicting, demands on prey phenotypes and particularly the morphology of the tail. In this evolutionary scenario, individual phenotypes supporting both quick propulsive movements for escape and steady steering needed for navigating towards a food source are ideal. Therefore, we expected that there would be a trade-off between performance in predator-avoidance and foraging. An individual that was very sensitive to predators, for example, would have a somewhat overactive escape reflex, interfering with its ability to hold station near a food source.

E. Random Mutation and Random Mating

All three traits were coded as continuous, quantitative diploid polygenes with independent assortment and no recombination. Genotypic values were mapped directly onto phenotype, with a narrow-sense heritability of one. From the diploid parental genotypes, haploid gametes were created by first halving the value of the genotype and then randomly mutating the haploid value using a Poisson distribution weighted to make mutations of greater than ± 25% of the phenotypic range unlikely (less than 10%; see Table 1 for ranges). Gametes were randomly combined in a mating pool to produce six new diploid genotypes of the offspring. The new individuals were created by randomly combining two haploid gametes from the gene pool to form diploid offspring genomes.

F. Strength and Orientation of Selection

To calculate the strength of selection on the population each generation, we took the difference between the mean of each trait from the three parents selected to breed and the mean of each trait of the parental population. When this selection triplet [ΔN, Δb, $\Delta \zeta$] was plotted relative to the population mean of that generation [$\bar{N}$, $\bar{b}$, $\bar{\zeta}$], the two points delineated a selection vector pointing towards a local fitness maximum with the scalar representing the composite strength of selection. The vector difference between the selection vector and the change in means between the parental and offspring generations, which can be viewed as the evolution vector, is caused by random effects, namely mutation and genetic drift.

G. Correlated Evolution via Eigen Decomposition

By design, all of the genetic variance of the three traits is additive. Thus, in each generation, we can calculate the genetic variance-covariance matrix, called the G matrix [2],

of the three traits in our population. Because selection can only act on variable traits and additive genetic variance is required for narrow-sense heritability, evolutionary changes in the *G* matrix show how selection and random effects sculpt the genetic make-up of the population as a whole. For each generation, we calculated the variances and covariances of the traits and all pairwise combination of traits, a process that yielded a 3x3 *G* matrix. We then computed an eigen decomposition of each *G* matrix (Mathematica, version 6.0, Wolfram, Inc). The first eigenvector, which by definition includes most of the system's variance (58 to 91% in this study), was used to summarize changes in the 3x3 *G* matrix.

H. Statistical Analysis

Evolved trait values for 30 genotypes (n = 30 per trait; 6 genotypes x 5 generations) were tested for normal distribution using a Shapiro Wilk W test (JMP, version 7, SAS Institute). Only *b* was normally distributed, and it had equal variances across generations (Levene and Bartlett tests). Thus we ran a one-way ANOVA on *b* with generation as the main effect. Since various transformations failed to make the distributions of *N* and ζ normal, we ran nonparametric Kruskal-Wallis rank sums tests, with generation as the main effect.

To investigate the robots' biomechanical performance we examined the relation of *u* and *a* to *N* and *b*. We chose *N* and *b* because both phenotypes are involved in the mechanics of propulsion. Both *u* and *a* were normally distributed. We regressed both *u* and *a* onto both *N* and *b* using a standard least-squares model. From the evolutionary trials, we also ran one-way ANOVAs of *N* and *b* with fitness rank as the main effect. Both tests were conducted in JMP (version 7, SAS Institute).

III. Results

Our predator and prey robots successfully produced chase, escape, and forage behaviors (Fig. 2) upon which selection acted over five generations. Of the three phenotypic targets of selection (Fig. 3), only the number of vertebrae, *N*, evolved directionally over five generations (Kruskal-Wallis, $p = 0.0429$; $\chi^2 = 9.8574$). Neither tail span, *b* (ANOVA, p = 0.8967; F = 0.2665), nor predator detection threshold, ζ (Kruskal-Wallis, $p = 0.1249$; $\chi^2 = 7.2368$), showed significant directional trends.

Neither mean swimming speed, *u*, nor peak acceleration, *a*, were significantly related to *b* or *N* in linear regression. In ANOVA, *u* varied significantly with fitness rank ($p < 0.0001$; adjusted $r^2 = 0.487$; $F = 7.6487$), but *a* did not ($p = 0.9491$; $F = 0.2243$) (Fig. 4).

Both strength and orientation of selection varied over generational time (Fig. 5). When viewed in two-dimensions, the three-dimensional [*N*, *b*, ζ] morphospace shows a complex fitness landscape. Orientation of the selection vectors suggest a single fitness maximum in the ζ-*N* plane and multiple or arc maxima in the *b*-*N* plane. Note also the relatively large impact on evolution of the random effects (difference between selection and evolution vectors).

Eigen decomposition of the six *G* matrices showed two evolutionary trends: (a) the variance of the population's first eigenvector decreased over time and (b) the trait with the largest coefficient in the first eigenvector changed from ζ to *b* over time (Fig. 6). The eigenvector and *G* matrix evolved.

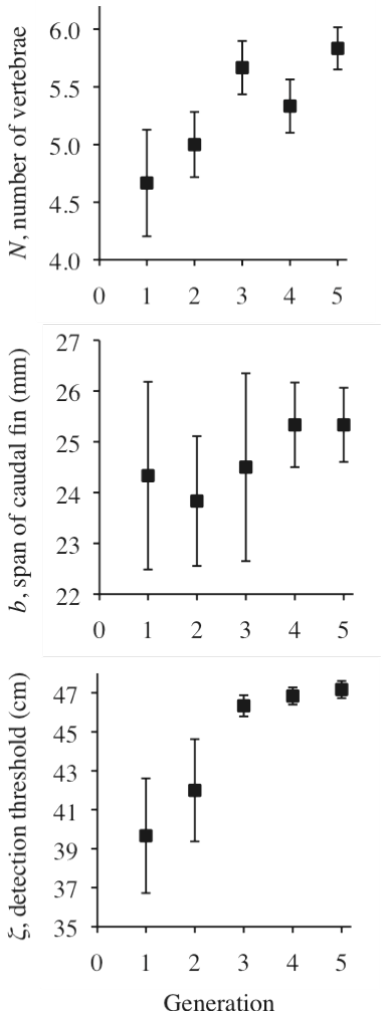

Fig. 3. Of the three available targets of selection, only vertebral number evolved directionally. The number of vertebrae showed a significant ($p < 0.05$) increase over generational time. Neither span of the caudal fin nor predator detection threshold were significant. Means ± standard errors of the mean (n = 6 for each mean).

IV. Discussion

Using robotic simulations of early fish-like vertebrates interacting as predator and prey (Fig. 2), we have shown that selection on the prey for enhanced foraging and predator avoidance is a plausible mechanism for positive directional evolution of the number of vertebrae, *N* (Fig. 3). However, in the same population of prey exposed to the same selection pressure, we find that neither the span of the caudal fin, *b*,

nor the predator detection threshold, ζ, evolve directionally. This was a surprising result, since we expected all three functionally-related traits to evolve in concert.

Since we determined the genetics of the system *a priori*, we can rule out genetic correlation as the cause of coupled stasis of b and ζ. Thus N was either the dominant or the only target of directional selection. While N was not correlated by regression with either mean swimming speed, u, or peak acceleration, a, we established an indirect link between N and u. We found that u was correlated with fitness rank (Fig. 4). Individuals of the highest rank, one to three, who were selected to breed every generation, had higher u values than the non-breeders, ranked four to six. Thus we have breeders who are fast and who evolve more vertebrae over generational time.

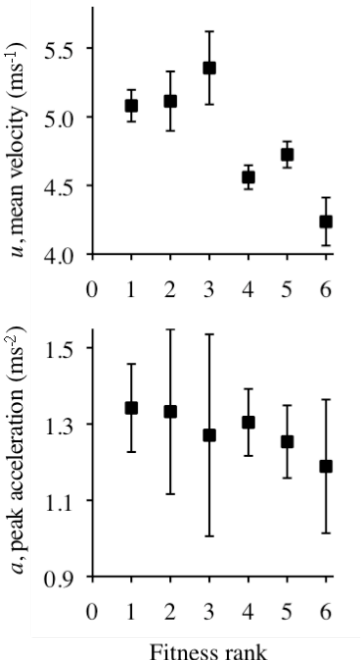

Fig. 4. Swimming velocity, but not acceleration, was correlated with fitness rank over five generations. Individuals with a fitness rank of 1 through 3 were permitted to breed each generation, and those individuals swam faster than the non-breeders. Means ± standard error of the mean (n = 5 for each mean).

Correlated evolution can also be examined using eigen decomposition of the population's G matrix, the genetic variance-covariance among the traits. Because the variance in the first eigenvector was dominated by a single trait in each generation, that trait evolved independently from the others (Fig. 6). However, the evolving trait changed. In generations one and two, ζ was the dominant trait. In generations three through six, b was the dominant trait. At the same time, the variance partitioned by the first eigenvector was shrinking. Additive genetic variance of a quantitative trait is required in order for that trait to respond to selection [2]. Traits under strong selection often show reduced variance over time. With this in mind, it appears that selection was operating initially on ζ and then, after two generations, switched to targeting b. The reduction in variance of these two traits without a corresponding shift in mean value (see Fig. 3) is evidence for stabilizing selection in the absence of directional selection.

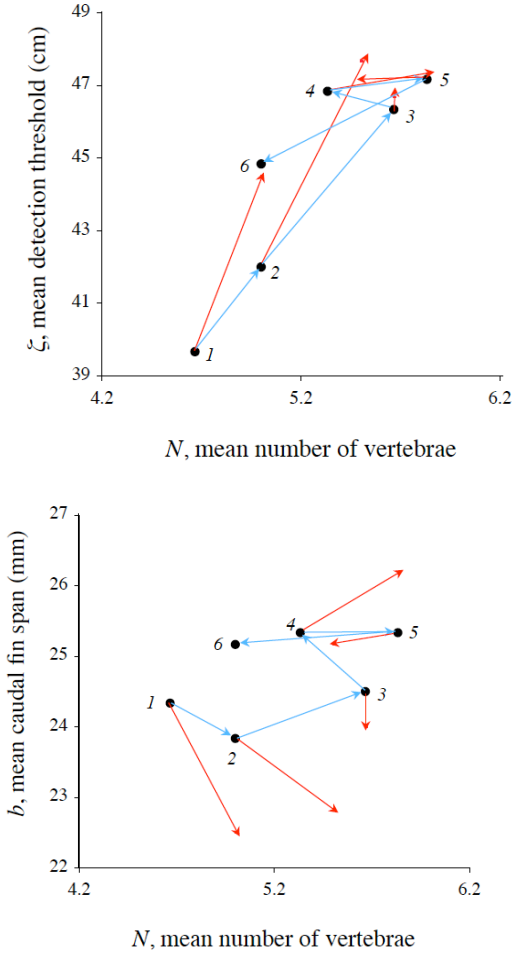

Fig. 5. Selection and the fitness landscape in morphospace. Blue vectors show the evolved change in the population mean over generational time, with generation enumerated. Red vectors show the strength and orientation of the average selection acting on the population. In any generation, the vector différence between the evolution and selection vectors is randomness (mutation and genetic drift). The selection vectors point towards local fitness maxima. The two-dimensional fitness landscape can be simple, with a single apparent minimum (towards the cluster of means in the upper right of the ζ-N morphospace, top), or complex, with either multiple peaks or an arc ridge (extending from below mean 1, around mean 3, and then between means 4 and 5 in the b-N morphospace, bottom).

Given that we have evidence that all three traits evolved independently, the evolution of the population can be interpreted (Fig. 5). In the ζ-N plane of morphospace, the population approaches what appears to be a single local maximum. The reduction in the size of the selection vectors as the population approaches the local maximum is most likely caused by the reduction in the additive genetic variance (see previous paragraph). Thus we predict that the population mean would likely stay close to this position [47 mm threshold, 5.7 vertebrae] in subsequent generations unless either the selection pressure changed or the magnitude of the random effects increased. In the b-N

morphospace plane, the evolution of the population is more complex, with selection vectors indicating either multiple fitness maxima or a curved ridge or arc of similar maxima. We cannot distinguish between the two with our limited resolution. In either case, a range of tail spans, *b*, appear to have high fitness, and we predict that the population would continue to move in the *b* dimension in subsequent generations.

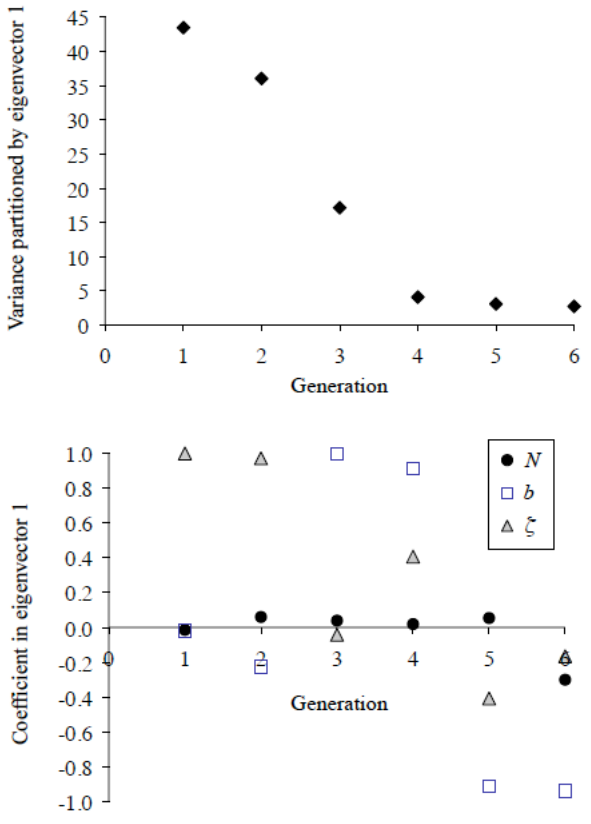

Fig. 6. Evolution of the *G* matrix of additive genetic variance-covariance of the three traits. Variance (top) partitioned by the first eigenvector decreased by an order of magnitude in three generations. This drop paralleled the switch from ζ to *b* as the dominant variable each generation. Reduction in variance of the *G* matrix is evidence for stabilizing selection of the dominant traits. Note that the traits show little correlation, which would be present as shared loading in a given generation.

We have demonstrated that biomimetic evolutionary analysis (BEA) is a useful approach for testing adaptation hypotheses about biological systems. Our robotic model simulation is fully embodied, unlike many ER and AL models, including our own [11], that are digital simulations. A drawback to digital simulations is that they have limited ability to model the dynamics of a physical environment. Since we are working with a particularly complex physical environment, one based on the coupled forces of a hydroelastic system in the body-water interaction, we take advantage of the fact that "... the world is its own best model" [3].

Nonetheless, caveats abound when using an embodied robotic simulation, or any simulation for that matter, to model adaptation. Our earlier BEA work on the evolution of axial skeletons [11, 12] can be criticized because it tested only a single selection pressure, presented only a single phenotypic target for selection, and overly simplified vertebrate structure and behavior. Those issues were paramount in the design of the new robotic simulation presented here. We succeeded in testing an additional selection pressure, presenting three phenotypic targets simultaneously for selection, and creating more complex robots in terms of structure and behavior. Given these significant changes, it is fascinating to see a similar result: that features of the axial skeleton, either spring stiffness [11, 12] or number of vertebrae (this study), evolve under different selection pressures.

Finally, we note that we have been careful to choose a selection pressure, predation, that is fundamental in the evolution of living fishes [7, 15] and embodied robots [4, 5, 16]. Future work entails the development of digital simulations of these robotic experiments to validate the results of the current experiments with larger population sizes and a greater number of trials.

V. Acknowledgment

We thank Kurt Bantilan, Sonia Roberts, Jonathan Hirokawa, Marianne Porter, Josh de Leeuw, Carl Bertsche, and John Vanderlee for their assistance. Ken Livingston, Charles Pell, Adam Lammert, and Joe Schumacher earn our gratitude for their inspiration of the robotic prototypes that led to this project. Finally, we thank the denizens of the Interdisciplinary Robotics Research Laboratory and the Abyss at Vassar College for their help in making this project happen.

References

[1] Arkin, R.C. (1998). Behavior-based Robotics. MIT Press: Cambridge, MA, USA.
[2] Bjorklund, M. (2004). Constancy of the G matrix in ecological time. *Evolution*, 58(6),1157-1164.
[3] Brooks, R. A. (1990). Elephants don't play chess. *Robotics & Autonomous Systems*, 6:3-15.
[4] Buason, G., Bergfeldt, N. and Ziemke, T. (2005). Brains, bodies and beyond: competitive co-evolution of robot controllers, morphologies and environments. *Genetic Programming and Evolvable Machines* 6(1):25-51.
[5] Buason, G. and Ziemke, T. (2003). Co-evolving task-dependent visual morphologies in predator-prey experiments. Pp 458-469 in Genetic and Evolutionary Computation Conference (Eds, Cantu-Paz et al.). Springer-Verlag: Berlin.
[6] Eaton (2001). The Mauthner cell and other identified neurons of the brainstem escape network of fish. *Progress in Neurobiology*, 63: 467-485.
[7] Endler, J. A. (1988). Sexual selection and predation risk in guppies. *Nature*, 332:593-594.
[8] Erwin, D. H., J. W. Valentine, and Jablonski., D. (1997). The origin of animal body plans. *American Scientis*, 85:126-137.
[9] Holland, N. and Chen, J. (2001). Origin and early evolution of the vertebrates: new insights from advances in molecular biology, anatomy, and palaeontology. *BioEssays,* 23:142-151.
[10] Koob, T.J. and Long, Jr., J.H. (2000). The vertebrate body axis: evolution and mechanical function. *American Zoologist,* 40:1-18.
[11] Liew, C.W., Root, R.G., Long, J.H. Jr., Koob, T.J. and Cummins, M. (2007). Using artificial organisms to study the evolution of backbones in fish. *Proceedings of the 2007 IEEE Symposium on Artificial Life*, 108-114.

[12] Long, J.H. Jr., Koob, T.J., Irving, K., Combie, K., Engel, V., Livingston, N., Lammert, A. and Schumacher, J. (2006). Biomimetic evolutionary analysis: testing the adaptive value of vertebrate tail stiffness in autonomous swimming robots. *Journal of Experimental Biology,* 209(23):4732-4746.

[13] Nolfi, S. and Floreano, D. (2000). *Evolutionary Robotics: The Biology, Intelligence and Technology of Self-Organizing Machines*. Cambridge MA: MIT Press.

[14] Purnell, M. (2002). Feeding in extinct jawless heterostracan fishes and testing scenarios of early vertebrate evolution. *Proceedings of the Royal Society London, B*, 269:83-88.

[15] Reznick, D. N. and Endler, J. A. (1982). The impact of predation on life history evolution in Trindadian guppies (*Poecilia reticulata*). *Evolution*, 36:160-177.

[16] Wischmann, S., Stamm, K. and Worgotter, F. (2007). Embodied evolution and learning: the neglected timing of maturation. *Lecture Notes in Computer Science*, 4648, 284-293.